Design and Implementation of the GPS Subsystem for the Radio Aurora Explorer

Sara C. Spangelo[a], Matthew W. Bennett[a], Daniel C. Meinzer[a], Andrew T. Klesh[a], Jessica A. Arlas[a], James W. Cutler[a]

[a] *University of Michigan, 1320 Beal Ave, Ann Arbor, MI 48109*

Abstract

This paper presents the design and implementation of the Global Positioning System (GPS) subsystem for the Radio Aurora eXplorer (RAX) CubeSat. The GPS subsystem provides accurate temporal and spatial information necessary to satisfy the science objectives of the RAX mission. There are many challenges in the successful design and implementation of a GPS subsystem for a CubeSat-based mission, including power, size, mass, and financial constraints. This paper presents an approach for selecting and testing the individual and integrated GPS subsystem components, including the receiver, antenna, low noise amplifier, and supporting circuitry. The procedures to numerically evaluate the GPS link budget and test the subsystem components at various stages of system integration are described. Performance results for simulated tests in the terrestrial and orbital environments are provided, including start-up times, carrier-to-noise ratios, and orbital position accuracy. Preliminary on-orbit GPS results from the RAX-1 and RAX-2 spacecraft are presented to validate the design process and pre-flight simulations. Overall, this paper provides a systematic approach to aid future satellite designers in implementing and verifying GPS subsystems for resource-constrained small satellites.

Keywords: CubeSat, Global Positioning System, GPS, Link Budget, Satellite Simulator, Nanosatellite, Subsystem design

1. Introduction

Onboard Global Positioning System (GPS) data enables coordination of global sensing systems and increases feature resolution in sensor systems [1, 2, 3]. Small satellite missions are increasing their use of GPS receivers to provide accurate and precise position and time information. Many of these missions conform to the CubeSat standard, a satellite form factor consisting of 10 cm cubes each weighing less than 1.3 kg [4, 5]. Over sixty CubeSats have been designed, built, and launched to perform novel science, technology demonstration, and educational missions to date [1]. Few of these missions have flown GPS subsystems because many currently available receivers consume a large percentage of available volume, power, and financial resources within these tightly-constrained missions [2]. Furthermore, maintaining proper GPS antenna orientation with respect to the GPS constellation requires the additional complexity of an attitude control system.

The primary contribution of this paper is the development of a design and testing methodology for CubeSat-based GPS subsystems. To date, there is little literature detailing techniques for designing, testing, and verifying complete GPS subsystems for small satellite missions. The relevance of this methodology is described throughout this paper in its application to the Radio Aurora eXplorer (RAX), a 3 kg CubeSat mission that requires GPS-based position and time synchronization [6]. RAX is the first of several CubeSat missions sponsored by the United States National Science Foundation (NSF) to study space weather. The primary objective of RAX is to study the formation of magnetic field-aligned plasma irregularities (FAI), which are dense electron clouds ranging from centimeters to kilometers in size that are known to disrupt tracking and communication between Earth stations and orbiting spacecraft [7]. RAX uses a bistatic radar configuration, as shown in Figure 1, where a ground-based radar illuminates FAI and a space-based receiver on RAX collects radar scatter. Two RAX satellites have launched with identical GPS subsystems. RAX-1 was launched into a 650 km altitude, 72° inclination orbit on November 19, 2010, and its mission is complete. RAX-2 was launched into a 410 by 820 km altitude, 101.5° inclination orbit on October 28, 2011, and is currently operational.

This paper also serves as design summary for future RAX data analysis. Each section of this paper presents successive stages in our methodology and its application to the RAX mission. First, Section 2 describes the RAX

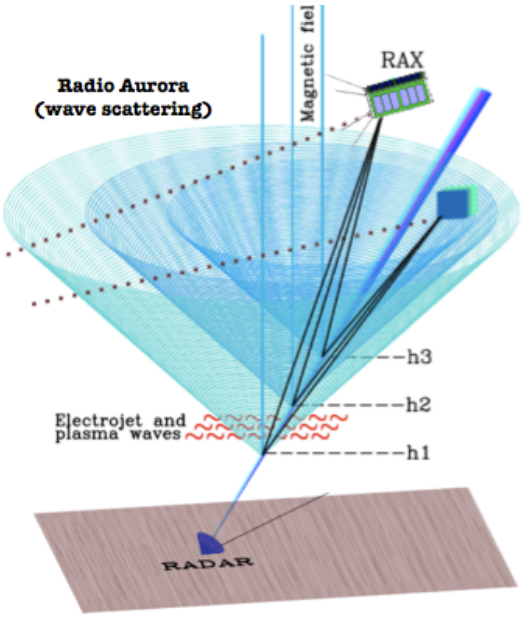

Figure 1: The GPS subsystem provides accurate position and time information during RAX measurements of ionospheric irregularities. RAX is the receiving system in a bistatic radar experiment that involves high power transmitters on the ground. The primary radar is located in Poker Flat, Alaska, USA. Radar pulses echo in conic patterns from the irregularities. The three cones represent scatter from irregularities at three different altitudes. The dotted lines are RAX flight paths through the experimental region where the satellites passes through the cones to receive radar echoes.

mission requirements and the constraints that impact the GPS subsystem. Section 3 reviews candidate GPS receivers and components applicable to the RAX mission. Section 4 details a link budget analysis and discusses simulations used to assess communication quality at representative satellite attitudes and orbital positions. Section 5 describes specific GPS performance metrics, tests, and results that verify system performance in terrestrial and simulated on-orbit environments. Section 6 provides a description of on-orbit performance and comparison to simulation results, which verifies the design approach and final design. The paper concludes with a summary and insights for the design of GPS subsystems for future missions.

2. Identification of GPS Subsystem Requirements and Constraints

The first step in any design process is assessing the functional requirements and constraints of the system under development. RAX has two functional requirements for the GPS subsystem that are derived from its mission science requirements [7]. First, received radar signals must be time-tagged with an accuracy of one microsecond. Second, the satellite location must be known within one kilometer accuracy during experiments. These two requirements are satisfied when a GPS fix is acquired. A *GPS fix* occurs when at least four GPS satellites are in view of the GPS antenna with signal strengths high enough for the receiver to acquire navigation data and calculate a position solution. Additional requirements are derived from the mission architecture and constraints, which are fundamentally shaped by the CubeSat platform. The GPS subsystem must satisfy the size, mass, and structural constraints of the CubeSat design specification so that it can fit inside the P-POD, the standardized launch vehicle interface [4]. The P-POD mechanical requirements state that no components may exceed the 6.5 mm clearance between the CubeSat edge and the inner walls of the P-POD, which thereby constrains the size and location of the GPS antenna. Thermal constraints must also be considered given the expected on-orbit temperature range of -40° to $+85^\circ$C.

RAX utilizes passive magnetic attitude control to ensure the radar receiver antennas are aligned for data collection over the ground radar station, as depicted in Figure 2. A permanent magnet aligns RAX with the Earth's magnetic field, and rotational energy is dampened with soft magnetic material. RAX oscillates about the magnetic field [8], impacting GPS constellation visibility. To achieve and maintain fix, a sufficiently strong signal strength is required to

satisfy the link budget. RAX attitude oscillations may degrade receiver performance. This places important constraints on the antenna selection, in that the antenna should have a wide beamwidth in order to minimize any negative impact from RAX attitude fluctuations.

Energy constraints for CubeSat missions limit the selection and operational duty cycle of the GPS subsystem. For example, the RAX satellites generate an estimated orbit-average of 5.1 W with a nominal power draw of 1.2 W. The power consumption of typical space GPS receivers ranges from 10 to 30 W [2]. Although it is possible for the RAX satellite to instantaneously provide this amount of power, the minimum duty cycle to satisfy the energy budget for these typical receivers would not satisfy mission requirements. Therefore, an alternative GPS receiver with low operating power and short acquisition times is required.

Programmatic and logistic requirements also constrained GPS system design. For example, the RAX mission had less than 11 months to design, build, test, and deliver the first satellite. The RAX team developed two vehicles (RAX-1 and RAX-2) in under 18 months with a fixed budget of $1M USD. This required a readily available receiver since there was insufficient time to develop one in-house.

A regulatory challenge for receivers in space is the removal of the Coordinating Committee for Multilateral Export Controls (CoCom) restrictions. The restrictions, enforced by the U.S. Department of Commerce, require that all exportable GPS products have performance limitations. The limitations enforce that the satellite measurements and navigation results such as position, raw code, and carrier measurement, will disable when the receiver's altitude and/or velocity limits are reached. [1] Some manufacturers disable tracking when both limits are reached while others disable tracking when one of the limits is reached. Not all receiver vendors are able to do this, resulting in a limited number of possible receivers.

3. Component Selection Design

The second step is to research designs and options for the primary components of a GPS subsystem: the receiver, the antenna, the low noise amplifier (LNA), and the supporting interface circuitry.

3.1. Receivers

Space GPS Receivers (SGRs) are designed for use in orbit, and typically have greater reliability and performance over terrestrial units. The BlackJack GPS Receiver, developed by the Jet Propulsion Laboratory, is flying onboard the Gravity Recovery And Climate Experiment (GRACE) satellites to provide accurate relative spacecraft position estimates to within 1 mm [2, 9]. Additional SGRs developed for small satellites by Surrey Satellite Technology Ltd (SSTL) and the European Space Agency (ESA) have flight heritage on missions like PoSAT-1 [10]. Unfortunately, a low-cost SGR with flight heritage or sufficient ground testing was not available during RAX mission development. SGRs available at the time of spacecraft construction had capabilities beyond RAX requirements, and resulted in two to three orders more magnitude in cost. Also, these units were not compatible with the RAX structural and mass constraints.

Several terrestrial receivers have been tested and operated in space. The CanX-2 nanosatellite, a mission developed by the University of Toronto Institude of Aerospace Studies, flew a NovAtel OEM4-G2L with CoCom constraints removed. It launched into low Earth orbit (LEO) in April 2008 and the GPS subsystem functioned successfully. During operation, the 1-σ position errors averaged less than 30 meters, and the errors were consistently biased in the radial direction [11]. The receiver's troposphere correction was not turned off, which accounted for approximately 10-20 meters of error. The magnitude of the errors was largely a function of the geometry of the satellite position and antenna relative to the GPS constellation. An algorithm was developed that combined the Simplified General Perturbations Satellite Orbit Model 4 (SGP4) orbit propagator, intermittent GPS orbital information, and Two Line Elements (TLEs) and then injected the estimated position into the receiver to improve GPS performance [3, 11, 12].

Both RAX CubeSats flew the terrestrial NovAtel OEMV-1-L1 GPS receiver, which had sufficient flight heritage and performance specifications. Firmware was upgraded to remove CoCom limits and improve space operations including removal of the troposphere model and extension of the Doppler window in order to assist with tracking at high velocities [2]. The receiver satisfied mission constraints and was very economical, costing less than 2% of the

[1] The altitude limit is 18 km and velocity limit is 0.25 km/s.

$150,000 USD budgeted for engineering design and flight unit hardware. The form factor and mass were compatible with the RAX requirements; it measured 46 mm x 71 mm x 10.3 mm and weighed 21.5 grams. Power consumption was 1.1 W and well within the power budget for RAX.

3.2. Antenna and LNA

The antenna provides visibility to the GPS satellite constellation, and the LNA amplifies received signals to the appropriate levels required by the receiver. In the literature, no specific discussion was found describing GPS antenna selection for satellites in LEO. However, Gao et al. discuss important interactions between antennas and modern small spacecraft and provide an overview of existing antenna design options [13]. Ortigosa et al. use simulation tools to experimentally verify the performance of patch antennas, helical antennas, and conical spiral antennas for space applications [14]. For the RAX mission, three common antenna design types from previous missions were considered: helical, monopole, and patch antennas.

The quadrifilar helical antenna is a double loop structure with good circular polarization properties [15]. With a spinning dipole across two orthogonally phased loops, this antenna generates a broad beamwidth with a cardoid shape as a far-field pattern. This broad pattern enables viewing of GPS satellites at low elevations relative to the antenna ground plane (where they spend most of their viewable time), despite having a lower peak gain as compared to more directional antennas. An example of this type of antenna is the GeoHelix-S, developed by Sarantel, which has a peak antenna gain of 0 dB, a beamwidth of approximately 120°, and an integrated LNA gain of 24 dB. Palmsat, a 1 kg satellite built by SSTL and students at the University of Surrey, selected this antenna due to its compact dimensions and sufficient gain [16]. However, that mission will not fly and has been superseded by the STRaND-1 mission which is flying a patch antenna to improve expected performance. In general, quadrifilar helical antennas have sufficient gain and a broad pattern for use in LEO. However, for the RAX mission, they did not easily fit within the structural constraints and would have required a deployment mechanism.

The monopole antenna is a dipole cut in half with a ground plane backing. It provides a toroidal antenna pattern with a null along the boresight direction. Additionally, it permits tracking of GPS satellites even at negative elevations, which are angles below the local horizontal reference. This is possible on-orbit but not in terrestrial applications. Monopoles are low-cost and easily constructed in-house. As an example, the PCSat mission (10 kg), launched by the United States Naval Academy, used a quarter wavelength monopole antenna. Their antenna was mounted on the corner of the cubic structure, since there was no available surface area to accommodate a more highly desired patch antenna [17]. The antenna and LNA combination had low gain, which resulted in lower than normal signal-to-noise ratios (SNRs) and poor GPS signal acquisition.

The patch antenna, also called a rectangular microstrip antenna, consists of a single metal patch over a ground plane and has a hemispherical antenna pattern. There are many commercially available patch antennas that satisfy the CubeSat form factor. The CanX-2 mission successfully flew the AeroAntenna AT2775-103 dual frequency (L1/L2) patch antenna with a 26 dB LNA, and successfully tracked and acquired GPS fix on-orbit [11].

The Antcom L1 GPS patch Antenna P/N 1.5G15A was selected for RAX due to its performance advantages over the monopole antenna, its satisfaction of the structural requirements, and initial estimates of subsystem performance. An integrated LNA provides 33 dB of gain, and the antenna has a 3 dB beamwidth of 103°. The antenna is 3.8 square centimeters with a mass of 42.5 grams and is vibration tested to over 30 Gs.

The location and orientation of the GPS antenna relative to the spacecraft is another design decision that must be considered. Poor antenna location can negatively impact the GPS subsystem performance. The RAX team installed the GPS antenna on the -Z surface of the spacecraft (see Figure 2) such that the passive magnetic system points the antenna toward the GPS constellation prior to, and during, the time it passes through the experimental zone over Alaska. The antenna mounting system was recessed into the structure to satisfy CubeSat P-Pod interface clearance requirements. Measurements in an anechoic chamber showed that this did not impact antenna performance. The integrated antenna on the RAX spacecraft is shown in Figure 3.

3.3. Position and Time Board

The receiver is mounted on a Position and Time Board (PTB) designed and built at the University of Michigan to provide power and communication interfaces, as shown in Figure 3. For ground testing, the receiver's Universal Serial Bus (USB) connection is accessible and a small breakout port allows direct probing of receiver signals. Primary communication with the flight computer is through a Serial Peripheral Interface (SPI) bridge to the Universal

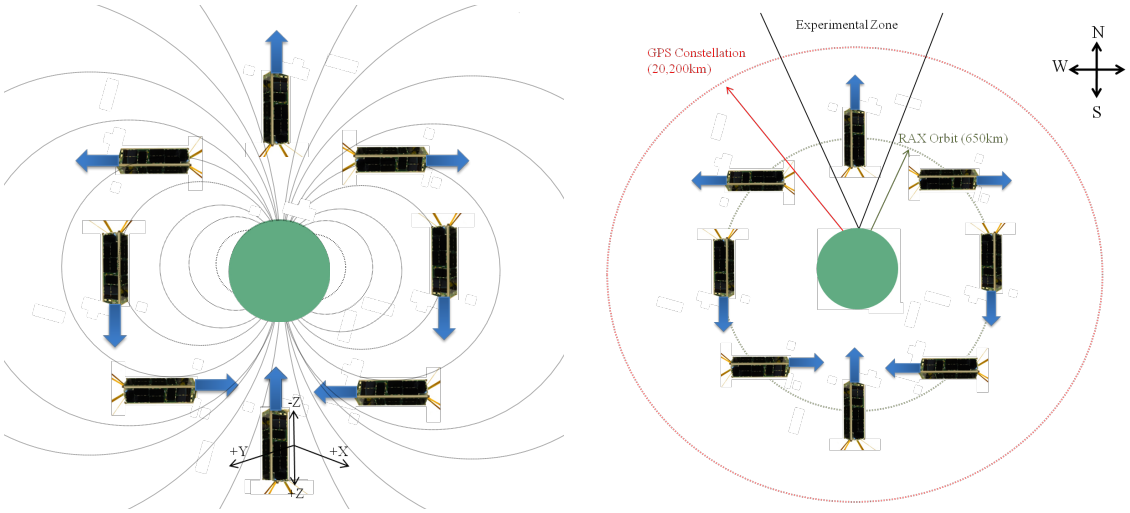

(a) Magnetic field lines

(b) RAX orbit, GPS orbit, and experimental zone

Figure 2: An approximation of RAX's orbit and orientation relative to the magnetic field and the orbits of the GPS constellation. RAX's attitude is passively controlled; its Z-axis is aligned with the Earth's magnetic field using a permanent magnet. The RAX-1 and RAX-2 orbits are inclined and the RAX-2 orbit is not circular, as described in the text. The schematic is not to scale.

Asynchronous Receiver/Transmitter (UART) interface on the receiver. The bridge also buffers UART data from the receiver and thus eases the computing load on the flight computer. The receiver's second UART is provided to the main satellite signal bus for monitoring by other subsystems. Signal isolators and power control circuitry isolate the PTB when the GPS subsystem is turned off. The receiver outputs a pulse-per-second (PPS) to the main satellite bus that is accurate to within 1 microsecond of GPS time. A low-power, real-time clock provides coarse timing and an auxiliary PPS for redundancy in case of receiver failure or planned power outages. As recommended by NovAtel, the receiver is enclosed in an anodized aluminum box for thermal and electromagnetic shielding.

4. GPS Link Analysis

The next step in this methodology is thoroughly predicting on-orbit performance of the GPS subsystem since only estimates were used during component selection. First, a link budget is developed to calculate the expected received signal strength at the RAX GPS receiver. The budget is assessed under best and worst case static RAX attitude

Figure 3: RAX-1 GPS Subsystem Hardware. On the left, the Antcom antenna is installed into RAX-1 engineering design unit. On the right, the Position and Time Board (PTB) is shown before encapsulation.

conditions in order to determine if the link is satisfied and how the two scenarios differ in expected performance. Second, the link budget is implemented with dynamic simulations to assess the visibility and expected signal strength of the GPS constellation as received by RAX during representative orbits. This analysis considers realistic satellite orbit, attitude, antenna gain pattern, and signal losses.

4.1. Analytical Link Budget

An analytical link budget is useful for calculating expected received power and carrier-to-noise spectral power density ratios (C/N_0) for the GPS subsystem. The power received by the GPS antenna, P_r, is defined in the logarithmic form of the link equation given below [18].

$$P_r = P_t + G_t + L_s + L_a + L_p + G_r \tag{1}$$

The transmit power and antenna gain, P_t and G_t, respectively, are characteristic of the GPS satellite. L_s is the space loss which varies dynamically throughout the orbit and is defined,

$$L_s = \left(\frac{\lambda}{4\pi S}\right)^2, \tag{2}$$

where λ is the wavelength of the transmitted signal and S is the path length. L_a represents the atmospheric losses and L_p denotes the polarization losses. G_r is the gain of the RAX receive antenna.

The antenna-to-receiver line loss, L_l, occurs as the received GPS signal travels between the LNA and GPS receiver. The system noise factor, F_s, is a function of the LNA noise factor, F_{LNA}, the line losses, L_l, and the gain of the LNA, G_{LNA}. In Eq. 3, these factors are combined to compute F_s using Friis' formula [19]. F_s and F_{LNA} are dimensionless in Eq. 3. The system noise temperature, T_s, is computed in Eq. 4 and is a function of F_s, the industry standard for calibrating the noise figure (290 K), and the antenna noise temperature, T_a.

$$F_s = F_{LNA} + \frac{L_l - 1}{G_{LNA}} \tag{3}$$

$$T_s = 290\ (F_s - 1) + T_a \tag{4}$$

The C/N_0 of the GPS signal at the GPS receiver is computed in Eq. 5, where k_B is the Boltzmann constant.

$$C/N_0 = P_r - 10\log T_s - 10\log k_B \qquad [dB] \tag{5}$$

In accordance with conservative design practices, the link margin (the difference between C/N_0 and the minimum required carrier-to-noise spectral power density ratio, $C/N_{0,min}$, should be at least 3 dB [18].

During experiments over Alaska, the RAX attitude control system points the GPS antenna in the zenith direction (radially away from the Earth). GPS satellite position in the constellation then determines best and worst case geometric scenarios for link budget analysis. The best case occurs when the GPS satellite is in the boresight direction of the RAX receiver antenna, which is 90° from the GPS antenna ground plane, as shown in Figure 4. The worst case occurs when the GPS satellite is at low elevation with respect to the ground plane, where the GPS receiver antenna gain decreases. The GPS transmit antenna gain is equivalent in both geometric cases [20]. The link budget analysis for these two scenarios for the RAX-1 spacecraft is shown in Table 1.

The NovAtel specifications indicate that the threshold for an acceptable GPS signal is $C/N_{0,min}$ = 35 dB·Hz [21]. Both cases presented in Table 1 satisfy the link margin requirement ($C/N_0 - C/N_{0,min} = G_M > 3$ dB), verifying that the GPS subsystem should be capable of acquiring and maintaining GPS fix in the space environment when four satellites are in view. The link budget was repeated for the RAX-2 orbit, where the minimum and maximum range distances were extracted from STK because of the more complex orbit. The worst-case scenario resulted in a maximum range of 28,200 km with G_M = 5.4 dB, and a minimum range of 21,900 km with G_M = 14.7 dB, both of which satisfied the link requirements.

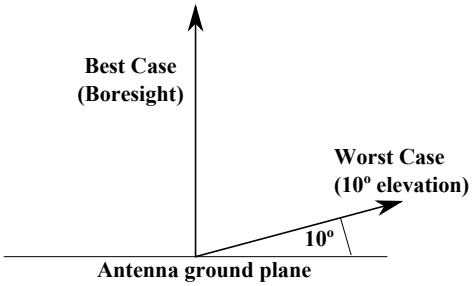

Figure 4: RAX GPS link budget best and worst case antenna orientations relative to GPS constellation.

Table 1: RAX-1 GPS link budget for average and best case scenarios.

Link Budget Parameter	Symbol	Worst Case (10° elevation)	Best Case (90° elevation)	Units	Source
Frequency	f	1.57542	1.57542	GHz	L1 GPS, Ref. [22]
Wavelength	λ	0.19	0.19	m	
GPS Transmitter Power	P_t	11.1	11.1	dBW	
GPS Transmit Antenna Gain	G_t	13.1	13.1	dBi	
Propagation Path Length	S	24,436	19,550	km	Geometry
Space Loss	L_s	-184.2	-182.2	dB	Eq. 2
Receive Antenna Gain	G_r	-2.5	4.6	dBic	Antenna gain pattern [23]
Polarization losses	L_p	-0.25	-0.25	dB	Ref. [23]
Atmospheric losses	L_a	0	0	dB	No atmosphere at 650 km
Antenna-to-receiver Line Loss	L_l	-2.0	-2.0	dB	Measured loss
Received Power (at the LNA)	P_r	-162.66	-153.62	dBW	Eq. 1
LNA Gain	G_{LNA}	33	33	dB	Ref. [23]
LNA Noise Figure	F_{LNA}	2.6	2.6	dB	Ref. [23]
System Noise Figure	F_s	2.6	2.6	dB	Eq. 3
Antenna Noise Temperature	T_a	30	30	K	Ref. [18]
System Noise Temperature	T_s	267.8	267.8	K	Eq. 4
Carrier-to-Noise Spectral Power Density Ratio	C/N_0	41.66	50.70	dB·Hz	Eq. 5
Minimum C/N_0	$C/N_{0,min}$	35	35	dB·Hz	Ref. [21]
Link Margin		6.7	16	dB	$C/N_0 - C/N_{0,min}$

4.2. Simulations

To verify the expected performance for representative spacecraft orbits and RAX attitude, a simulator calculates GPS link characteristics between the RAX GPS subsystem and the GPS constellation. This assesses performance as a function of orbit latitude and throughout the RAX experimental zone (54-72° latitude). The simulations assume the GPS link has already been acquired and is maintained. The reason for this assumption is to isolate the effects of latitude on the link characteristics (tests in Section 5.2 investigate GPS start-up times as a function of latitude).

The link budget simulations were performed using scripts in Matlab interfaced with Systems Tool Kit (STK). The simulation model included expected orbital position and orientation of the RAX satellite, antenna gain patterns, and signal losses from both the GPS satellite transmitter and GPS subsystem. STK propagated the RAX-1 and RAX-2 orbits and estimated attitude based on the predicted orbital parameters, magnetic field alignment, and spin rate (10° about the Z axis), while the STK/Communications module dynamically evaluated the link budget throughout simulated orbits.

These simulations assessed the number of GPS satellites in view with sufficiently strong signals ($C/N_0 \geq 35$ dB·Hz) throughout a representative scenario. The average, minimum, and maximum number of GPS satellites that satisfied the link budget as a function of latitude are plotted for RAX-1 and RAX-2 in Figure 7. The RAX-1 satellite

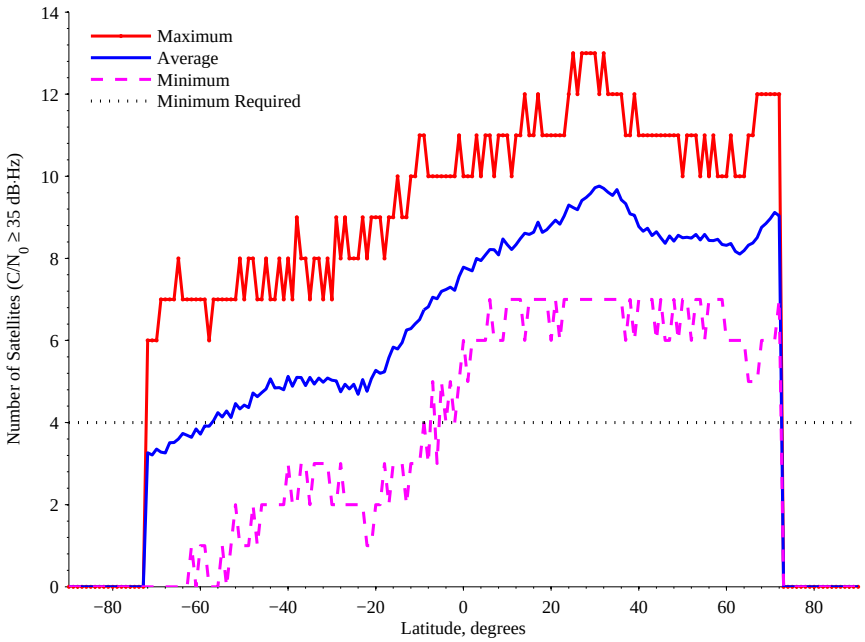

(a) RAX-1, circular orbit with orbital altitude= 650 km, inclination = 72°

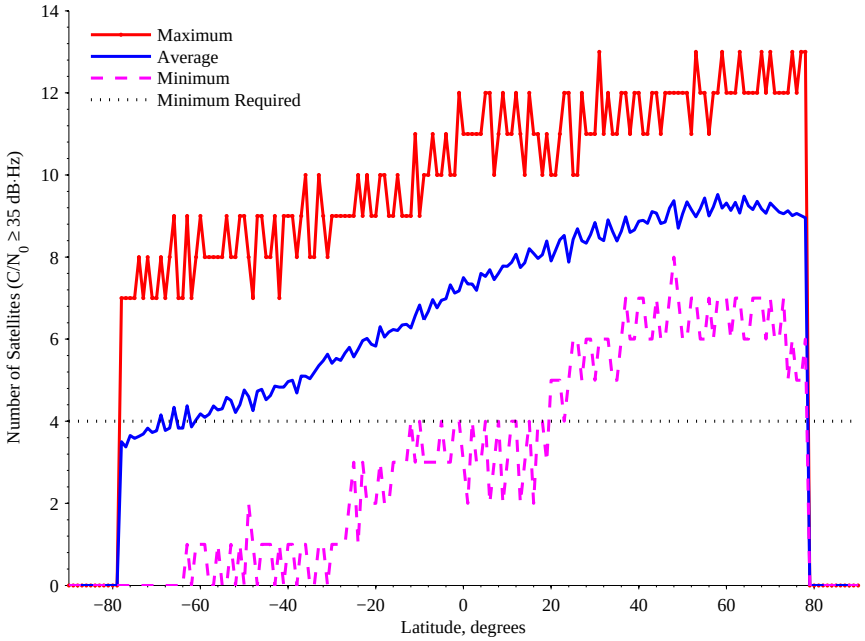

(b) RAX-2, orbital perigee= 410 km, orbital apogee= 820 km, inclination= 101.5°

Figure 5: Results of a dynamic link budget analysis for the RAX satellites performed using integrated Matlab and STK tools for one week scenarios. The plot shows the number of satellites in view with required $C/N_0 \geq 35$ dB·Hz as a function of orbit latitude.

has a 72° inclination orbit, thus GPS link results are confined to latitudes ranging from −72° to 72°. RAX-2 has an orbital inclination of about 101.6° and therefore the orbit latitude range is confined to approximately −78° to 78°.

In the simulations, as the latitude decreased, the receive antenna began to point toward Earth due to RAX's

magnetic alignment (see Figure 2), limiting the number of visible GPS satellites. RAX-2 tended to yield higher maximum number of satellites, particularly at low (<10°) and high (>40°) latitudes. The latitude where the average number of satellites drops below the threshold is relatively constant for both satellites (approximately -60°). The latitude where the minimum number of satellites crosses this threshold occurs at approximately -5° for RAX-1 and approximately 20° for RAX-2, which can be attributed to their different orbital geometries (RAX-2 has a lower orbital perigee where the Earth restricts the field of view and has a smaller orbital inclination). The variability between the minimum and maximum number of satellites at a particular latitude in Figure 7 is due to the diversity of the configuration (altitude and orientation) of the RAX-1 or RAX-2 spacecraft relative to the GPS constellation during the one week simulation. The average difference between the minimum and average and maximum and average number of satellites in view was approximately 2.1 and 2.2 for RAX-1 and 2.9 and 3.1 for RAX-2. RAX-2 has greater variability due to its larger orbital eccentricity and resulting altitude range.

According to the simulations, a GPS fix should be maintained when RAX-1 is at latitudes greater than -5° and RAX-2 is at latitudes greater than 20°, which encompasses the experimental zone. Thus, this analysis verifies that the GPS subsystem design satisfies mission requirements for both RAX-1 and RAX-2 orbits. Furthermore, the variability of results over different orbits has been identified.

5. Pre-flight Integration and Testing

GPS receiver output logs provide valuable data for evaluating performance. The receiver can output time and position estimates, uncertainties, solution status, and GPS satellite data including the C/N_0, elevation angle, and azimuth angle [21]. The number of satellites in view and their signal strengths are key metrics used to evaluate if the receiver is likely to obtain, maintain, or lose fix. The following metrics are derived from the output logs used to evaluate GPS performance:

- *Pulse-per-second (PPS) timing accuracy:* The receiver outputs a PPS accurate to within 1 μs of GPS time when the receiver is fixed to the constellation. The time status of the receiver at this point is called *finesteering*. When the receiver loses fix, the PPS will drift due to oscillator inaccuracies in the receiver. Measuring the PPS under various conditions characterizes the receiver clock performance.

- *Time to first finesteering (TTFS):* TTFS is the time it takes for the receiver to achieve finesteering after it is powered on. For the RAX mission, the TTFS indicates the minimum amount of time the receiver must be powered on prior to performing an experiment. A short TTFS is desirable to minimize power consumption for a power-constrained mission like RAX. The receiver can power on in three configurations: *cold*, *warm*, and *hot*. In a *cold* start, the receiver has no almanac (knowledge of the GPS satellite constellation), no ephemeris (recent receiver position information), and no approximate position or time. A *warm* start is when no recent ephemeris information is available, but the almanac is stored by the receiver and an approximate position and time is injected by the user via the data interface. A *hot* start is when the receiver has an almanac, a recent ephemeris saved, and an approximate position and time is injected into the receiver. The receiver should locate and obtain a fix to the GPS constellation more quickly during *warm* or *hot* starts since it has more tracking information.

- *Time to first almanac (TTFA):* In the case of *cold* starts, the receiver does not have an almanac, therefore the time to acquire the first almanac is an important performance metric. Valid almanacs are required to obtain GPS fix, and the quality of the almanac degrades over time. Almanacs older than 26 weeks are deleted from the OEMV-1 (and the subsequent start will be a *cold* start). In the context of RAX, the TTFA is important the first time the GPS receiver is powered and after every almanac expiration.

- *Carrier-to-noise spectral power density ratio (C/N_0):* The C/N_0 ratios of the GPS satellites in view of RAX's GPS antenna provide information about the strength of the received signal, and a minimum value, $C/N_{0,min}$, is required to obtain GPS fix.

- *Position Accuracy:* The GPS receiver provides an estimate of the position and velocity errors in the form of $1-\sigma$ error estimates in the Earth Centered Earth Fixed Cartesian coordinate system. This information is used to

verify if the one-kilometer position accuracy requirement for the RAX mission is satisfied, and to characterize uncertainty as a function of time status, orbital position, spacecraft attitude, and geometry relative to the GPS constellation.

These metrics were measured at three levels of integration to assess the impact of individual components on overall GPS performance:

1. A GPS antenna was mounted on the roof of the laboratory building in Ann Arbor, Michigan, USA, for an unobstructed view of the sky. It was connected to a receiver inside the laboratory. This configuration enabled testing of the receiver and antenna combination.
2. A portable, semi-integrated test apparatus was built consisting of a receiver, coaxial cable, antenna, PTB, and an electrical power system (EPS) with a battery power supply. This configuration enabled outdoor testing, characterization of different antennas, and initial assessments of electromagnetic noise interference.
3. The final level was the fully integrated satellite. This enabled full, end-to-end testing of the RAX GPS subsystem.

The GPS subsystems for both RAX spacecraft were tested in two environments. In the terrestrial environment, all three system integration stages were tested for GPS functionality. In the simulated orbit environment, a specialized GPS satellite simulator (GSS) tested the fully integrated spacecraft and individual GPS receivers. The remainder of this section discusses the GPS results from the tests at different stages of system integration in the two environments, using the performance metrics discussed above.

5.1. Terrestrial Tests

PPS timing was characterized using level one integration. First, the PPS accuracy and drift between two receivers was characterized. NovAtel reports the timing error is ≤ 20 ns for receivers with a GPS fix [21]. Timing differences were measured between two receivers having identical configurations, attached to the same antenna, and with GPS fix to test accuracy. The average time difference in rising edges of the PPS output was 10 ns and the maximum was 30 ns. This test ensures consistency between the two receivers, however does not account for biases in both the measurements and thus does not provide absolute accuracy information.

PPS timing drifts when the receiver loses fix due to inadequate GPS visibility or signal strengths. Signal loss was simulated by commanding the receiver to omit satellites during solution calculations. At 25° C, the PPS clock drifted at approximately 7.1 ns per second. Thus, within 2.3 minutes of losing GPS fix, the receiver drifts beyond the 1 μs accuracy requirement. Again, this test only takes into account relative drift between the receivers. Experimental analysis of the clock drift as a function of temperature was not performed due to time constraints and the lack of thermal test facilities near an antenna with constellation visibility. However, conversations with NovAtel and the basic testing indicated that the receiver tolerances to temperature change were known and drift could be estimated if a loss of lock occurred on-orbit during an experiment.

Results from TTFS and TTFA testing at integration levels one and two were consistent with the NovAtel specifications [21]. However, initial testing at the fully integrated level initially failed due to the receiver's inability to obtain a GPS fix. Debugging efforts revealed that the failure was caused by electromagnetic interference (EMI) generated by the receiver itself, in close proximity to the GPS antenna. This problem was mitigated by moving the receiver farther from the antenna, as shown in Figure 6, and adding EMI absorption material near the receiver. These two adjustments enabled receiver operation while fully integrated.

The integrated RAX satellites had an average TTFS of 85 seconds for warm starts, 112 seconds for cold starts, and required an average of 12.63 minutes to download an almanac. NovAtel reports that TTFS is 45 - 50 seconds for a warm start and 70 - 75 seconds for a cold start, and downloading an almanac requires 12.5 - 15 minutes [21]. There was no notable timing difference between warm and hot starts. This testing verified the proper GPS subsystem performance in a terrestrial environment.

5.2. Orbital Simulation Tests

There is a significant difference between operating GPS receiver in LEO relative to terrestrial usage [2, 24]. Proper GPS system characterization in the on-orbit environment requires testing with a GPS Satellite Simulator (GSS).

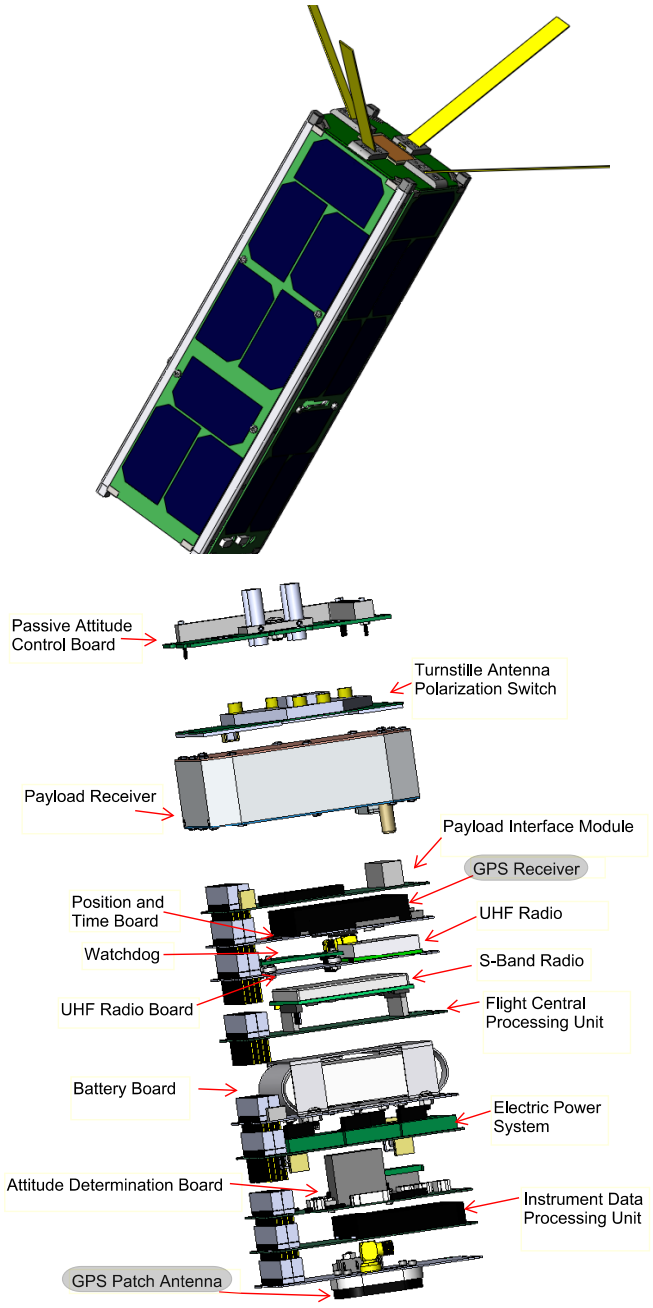

Figure 6: RAX-1 Computer Aided Design model. The fully integrated assembly is shown on the left and the assembly with internal boards only is shown on the right. The GPS components are shadowed. The boards have been re-arranged to mitigate noise interference issues.

Table 2: Results from testing integrated the RAX satellite in the GSS. The time to first finesteering (TTFS) and time to first almanac (TTFA) for expected start-ups (modified warm and cold starts) at different latitudes are shown. Modified warm starts did not have approximate time or position injected.

Test	Start Type	Valid Almanac	Latitude	TTFS	TTFA
1	Modified Warm	Yes	59.17°	1.93 mins	-
2	Modified Warm	Yes	53.05°	1.12 mins	-
3	Modified Warm	Yes	39.90°	0.77 mins	-
4	Modified Warm	Yes	15.69°	2.05 mins	-
5	Cold	No	15.69°	5.28 mins	12.77 mins

The GSS replicates expected orbital signal characteristics including ionospheric effects, negative viewing elevation angles with respect to the GPS constellation, and Doppler shift due to high relative velocities of the satellites. The RAX spacecraft was simulated throughout expected orbits with the magnetic control scheme in Figure 2. Testing of individual receivers prior to integration confirmed that CoCom limits had been removed.

Once each RAX spacecraft was fully integrated (level 3), TTFS and TTFA were measured under various operational environments and the results were as expected, see Table 2. The average TTFS for the cold starts in the GSS was 5.28 minutes, notably longer than the 1.87 minutes averaged by the terrestrial tests. This was expected since the receiver must search longer for GPS signals due to the Doppler shift. Average TTFA values were similar between terrestrial and GSS tests since downloading an almanac requires a continual fix and once fix is obtained, the time to download an almanac is independent of being in terrestrial or on-orbit conditions. Warm start tests with initial position injection were not performed since earlier testing indicated no performance improvement.

TTFS sensitivity to satellite position, in particular latitude, was measured. TTFS measurements for select latitudes are summarized in Table 2. The general trend in measurements are consistent with the simulated dynamic link budget analysis in Figure 7. In particular, the TTFS is related to the expected number of satellites in view as a function of orbit latitude. The shortest warm TTFS occurs at a latitude of 39.90° (Test 3), which coincides with a peak in the expected number of satellites in Figure 7. The longest warm TTFS occurs at a latitude of 15.69° (Test 4), which coincides with a dip in the expected number of satellites with sufficiently high signal strengths.

GSS testing showed sufficient number of GPS satellites with adequate C/N_0 values during the portions of the orbit where GPS fix is required. C/N_0 values were recorded for a representative orbit with the fully integrated RAX interfaced to the GSS. This average C/N_0 reported by the receiver was 49.5 dB·Hz. Note, this value is adversely affected by internal satellite noise sources, so only the essential subsystems were turned on during the test. This C/N_0 is greater than the required $C/N_{0,min}$ = 35 dB·Hz and consistent with the predicted link budget in Table 1.

The C/N_0 and number of visible satellites in view decrease when the satellite is in the southern hemisphere and approaching the South Pole. Loss of fix occurred when RAX's latitude fell below -67°, which corresponds with a significant decrease in the expected observed number of satellites, as shown in Figure 7. Loss of GPS fix lasted approximately 16 minutes of the 96.5 minute orbit. Once RAX's latitude increased to approximately -18°, the number of satellites in view and the C/N_0s recovered quickly, and GPS fix was obtained again.

During the simulations, estimates of error by the GPS receiver were well below the 1 km accuracy requirement. GPS position errors can be caused by a variety of sources, including ephemeris errors (±2.5 meters), satellite clock errors (±2 meters), multipath distortion (±1 meter), numerical errors ($\leq$ ±1 meter), and loss of fix [25]. The average error in the Earth-Centered Earth-Fixed (ECEF) X, Y, Z, and norm of all directions was 4.3, 4.6, 12.7, and 14.2 meters, respectively. The errors were relatively constant throughout the orbit except for large spikes (to a maximum norm of 250 m) immediately before GPS lock was lost.

Therefore, with both terrestrial and orbit simulation testing, the RAX GPS subsystem was found to be fully operational and capable of satisfying mission requirements.

6. Preliminary Flight Results

For both RAX spacecraft, GPS check-out was performed after achieving reliable tracking and communication with the spacecraft and preliminary subsystem check-outs. The RAX-1 receiver was first operated approximately

Table 3: RAX-1 and RAX-2 GPS flight test information. For Tests 1A and 1B, data was recorded immediately after being turned on. For Tests 2A and 2B, data was first recorded approximately five minutes after the receiver was turned on.

Spacecraft	Test	Date	Time Data First Recorded (UTCG)	NovAtel Log	Test Duration (mins)
RAX-1	1A	Dec 29, 2010	02:55:51	GPGSV	19.15
RAX-1	1B	Dec 29, 2010	16:05:45	BESTXYZ	5.11
RAX-2	2A	Nov 11, 2011	07:19:05	GPGSV	100
RAX-2	2B	Nov 12, 2011	18:39:05	BESTXYZ	100

one month after launch and the RAX-2 receiver was first operated approximately two weeks after launch. For both missions, the GPS check-out tests were successful; GPS lock was achieved and the system functioned as expected, satisfying the RAX GPS subsystem mission requirements. These tests confirmed successful operation of the full GPS subsystem, including the antenna, coax, LNA, receiver hardware and firmware, PTB, and all supportive systems. The success of the GPS tests verifies the design process presented in this paper.

Table 3 summarizes the dates, durations, and NovAtel user-specified logs for each GPS functional experiment performed by the RAX-1 and RAX-2 spacecraft. Approximately 9% of the data from Flight Test 2B was not successfully recovered due to data logging and download complications, and thus is not included in the analysis. The missing data was distributed over small intervals throughout the functional test, thus has minimal impact on the results as a function of time or latitude. GPS lock was maintained throughout the full test for Tests 2A and 2B. The ability to perform more extensive on-orbit tests was limited for RAX-1 due to a power system failure that resulted in an early mission termination [6]. There is also limited RAX-2 data due to on-board storage failure that prevents normal GPS data logging [26]. However, at the time of writing (Nov. 2012), GPS tests are planned in the near future using a new data storage approach.

To validate the simulations and provide flight data, pre-flight simulation data is compared to on-orbit data. In particular, flight test 2A (which contains C/N_0 data for a full orbit) is compared to link budget STK simulation results (described in Section 4.2) in Figure 7. For the test, satellite position was estimated using the TLE with the closest epoch to the time of the test and was propagated using an SGP4 model. The average number of satellites in view above $C/N_{0,min}$ was 9.2 satellites. In contrast to the link budget STK simulations, the number of satellites in view does not vary significantly as a function of latitude. Throughout the orbit, the GPS antenna has more satellites with $C/N_0 \geq 35$ in its field of view than expected. In particular, there is no dramatic decrease in the number of satellites in view and with $C/N_0 \geq 35$ as the latitude decreases. This is particularly true over the Southern hemisphere, where the GPS antenna is expected to be pointed directly at the Earth (see Figure 2), and thus have a limited view of the GPS constellation. There are two suggested causes for this observation. First, in the link budget STK simulations, it is assumed the RAX-2 spacecraft is magnetically field aligned however, preliminary attitude data and GPS data indicate that the RAX-2 spacecraft had not fully stabilized to its expected attitude scheme at the time of this test, see Ref. [26]. This may yield a different field of view of the GPS constellation, and possibly more spacecraft in view, particularly over the Southern hemisphere. Second, the antenna gain pattern may have been oversimplified. Preliminary anechoic measures suggest there may be gain below the RAX GPS antenna ground plane (i.e. at elevations $< 0^\circ$), which would result in a larger field of view. There is excess margin in the GPS link budget and the link budget was conservative relative to on-orbit results, thus it may be possible for GPS satellites below the horizon to satisfy the link budget.

Figure 8 compares the on-orbit C/N_0 data with the simulated link budget values for two example GPS satellites, which are each identified by a pseudo-random number (PRN). The general C/N_0 trends are similar for true orbit data and simulation for several of the satellites, such as PRN 31 in Figure 8(a). The true orbit C/N_0 values often exceed the expected simulation values, confirming the link budget approach is valid and conservative. For a handful of GPS satellites, the trends for the simulated and true orbit C/N_0 data are not in agreement, such as for PRN 15 in Figure 8(b). This demonstrates an example of the RAX-2 GPS antenna having a field of view that is different then to the attitude and antenna gain issues discussed above. Future work will investigate this further.

The errors from the GPS Flight Test 1B and 2B are summarized in Table 4. The reported errors for both GPS tests are significantly below the 1 km subsystem requirement. In addition, these errors were considerably better for RAX-2

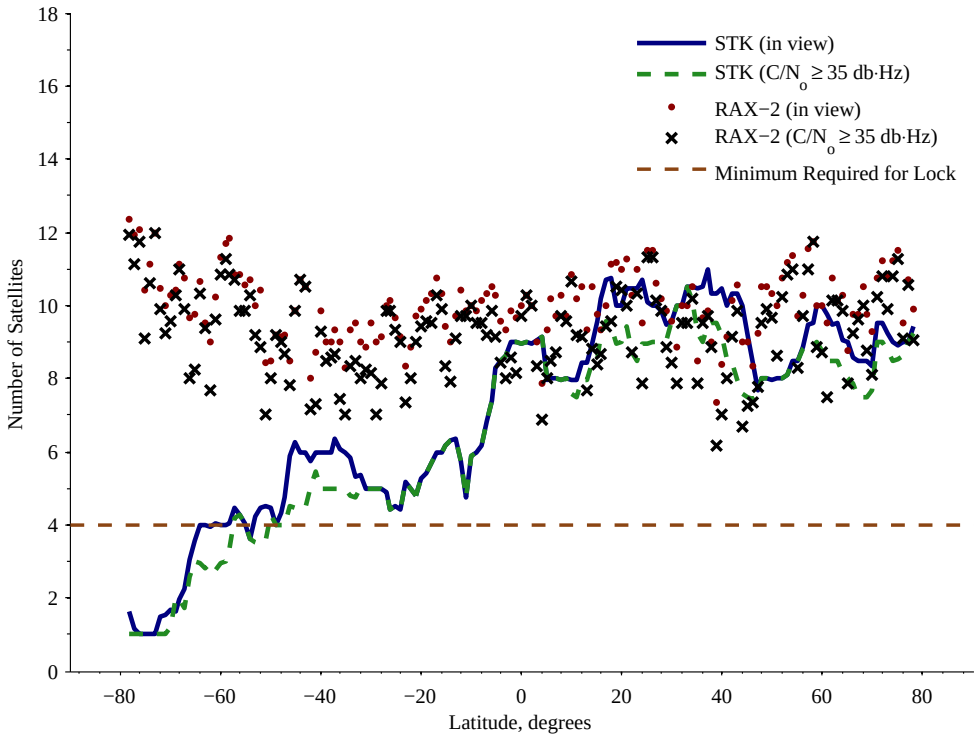

Figure 7: Comparison of RAX-2 on-orbit results with a dynamic link budget analysis using integrated Matlab and STK tools. The plot shows the number of satellites in view with required $C/N_0 \geq 35$ dB·Hz as a function of orbit latitude during a representative orbit.

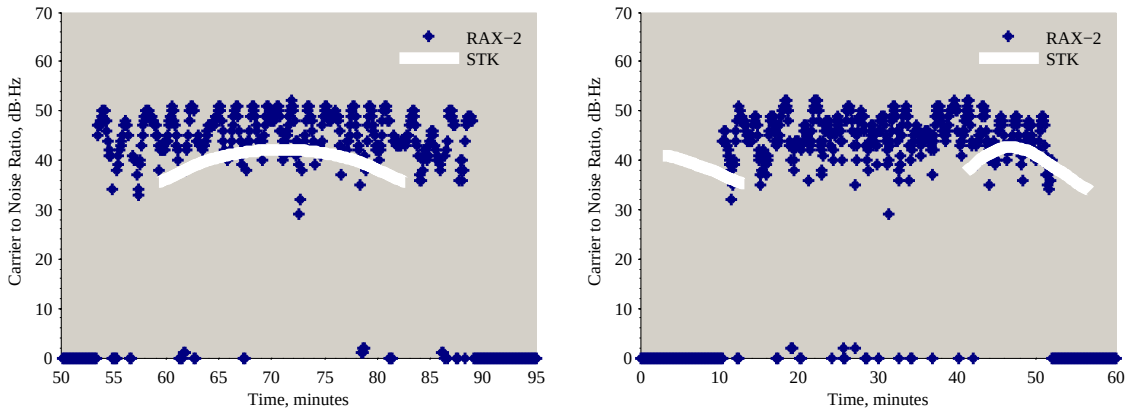

(a) GPS Satellite PRN 31

(b) GPS Satellite PRN 15

Figure 8: Comparison of on-orbit GPS data with STK simulation.

than for other CubeSat missions. For example, CanX-2 used a OEM4-G2L receiver which had position errors greater than 10 meters and the average errors were around 30 m when GPS fix was maintained [12]. Causes for these errors are described in Section 3.

Table 4: Average position and velocity standard deviation errors from GPS flight Test 2. R_2 and v_2 are the Euclidean norms of the error in the three position and velocity components (x, y, z).

	RAX-1 (Test 1B)		RAX-2 (Test 2B)	
Magnitude	R_2	v_2	R_2	v_2
Average Error	4.07 m	0.49 m/s	2.89 m	0.34 m/s

7. Conclusions

This paper described the design, analysis, and testing of the GPS subsystem for the RAX mission. Like many upcoming small satellite missions, the RAX mission required a GPS subsystem to provide accurate temporal and spatial information to satisfy the mission objectives. We outlined a general methodology for the design and implementation of a GPS subsystem that is applicable for future missions. The methodology enables development of a functional GPS subsystem for low Earth orbiting satellites that includes design decisions for the receiver, LNA, antenna, and supporting circuitry.

Several lessons were learned throughout the design and testing effort, but the most unexpected was the susceptibility of the receiver system to self-generated EMI. For future missions, we recommend early and systematic testing of the GPS subsystem throughout the integration stages to identify and mitigate EMI problems.

Preliminary flight results for both RAX-1 and RAX-2 spacecraft were presented. The results were compared to expected performance from pre-flight simulations and verified the design process and final design. The full flight results will be published in future work. Future research will include efforts to understand the errors between TLEs and GPS data, characterizing C/N_0 and position accuracy, and analyzing the sensitivity in start-up time to spacecraft latitude, GPS constellation geometry, and RAX spin rates.

Acknowledgements

Two of the authors, Matthew W. Bennett and Dr. Andrew T. Klesh, are now employed at the Jet Propulsion Laboratory (JPL), and their contribution to the work in this paper was completed prior to their JPL employment. We thank Dr. Eric Gustafson, John Springmann, Alex Sloboda, Ben Kempke, Allison Craddock, Eric Wustrow, Vijay Patel, Bill Woelk, and the entire University of Michigan RAX Team for their contributions. We also acknowledge Courtney Duncan, Erin Kahr, Jeff Dickson, NovAtel Industries, and AGI Support for their valuable insight and knowledge.

Finally, we acknowledge JPL, Orbital Sciences Corporation and The Aerospace Corporation for their valuable help, guidance, and use of their GSS facilities. This work was supported by NSF grant ATM-0838054 to SRI International and the University of Michigan. We thank the Natural Sciences and Engineering Research Council of Canada and Zonta International for their support.

8. References

[1] K. Woellert, P. Ehrenfreund, A. J. Ricco, H. Hertzfeld, Cubesats: Cost-effective science and technology platforms for emerging and developing nations, Advances in Space Research 47 (4) (2011) 663–684.
URL http://www.sciencedirect.com/science/article/pii/S0273117710006836

[2] O. Montenbruck, Performance assessment of the NovAtel OEM4-G2 receiver for LEO satellite tracking, Space Flight Technology, German Space Operations Center (GSOC) (2003).
URL http://www.weblab.dlr.de/rbrt/pdf/TN_0305.pdf

[3] M. Greene, R. Zee, Increasing the Accuracy of Orbital Position Information from NORAD SGP4 Using Intermittent GPS Readings, in: Proceedings of Conference on Small Satellites, Logan, UT, 2009.

[4] Cubesat Design Specification, Revision 12, The CubeSat Program.

[5] A. Chin, R. Coelho, L. Brooks, R. Nugent, J. Puig-Suari, Standardization Promotes Flexibility: A Review of Cubesats Success, in: Proceedings of 6th Responsive Space Conference, Los Angles, CA, 2008.

[6] J. W. Cutler, J. C. Springmann, S. Spangelo, H. Bahcivan, Initial Flight Assessment of the Radio Aurora Explorer, in: Proceedings of the 25th Annual Small Satellite Conference, Logan, UT, 2011.

[7] H. Bahcivan, M. Kelley, J. Cutler, Radar and rocket comparison of UHF radar scattering from auroral electrojet irregularities: implications for a nano-satellite radar, Journal of Geophysical Research 112 (A04204).
URL doi:10.1029/2006JA011900

[8] G. Park, S. Seagraves, H. McClamroch, A Dynamic Model of a Passive Magnetic Attitude Control System for the Rax Nanosatellite, in: Proceedings of the AIAA Guidance, Navigation, and Control Conference, Toronto, ON, 2011.
[9] R. Kroes, O. M. W. Bertiger, P. Visser, Precise GRACE baseline determination using GPS, GPS Solutions 9 (2005) 21–31. URL http://dx.doi.org/10.1007/s10291-004-0123-5
[10] M. J. Unwin, M. N. Sweeting, First results from PoSAT-1 GPS experiment, in: Proceedings of the 1994 National Technical Meeting of The Institute of Navigation, San Diego, CA, 1994.
[11] E. Kahr, O. Montenbru, K. OKeefe, S. Skone, J. Urbanek, L. Bradbur, P. Fenton, GPS tracking on a nanosatellite the CanX-2 flight experience, in: Proceedings of 8th International ESA Conference on Guidance, Navigation and Control Systems, Karlovy, Czech Republic, 2011.
[12] E. Kahr, S. Skone, K. OKeefe, Orbit determination for the Canx-2 nanosatellite using intermittent GPS data, in: Proceedings of ION GNSS, Portland, OR, 2010.
[13] S. Gao, K. Clark, M. Unwin, J. Zackrisson, W. Shiroma, J. Akagi, K. Maynard, P. Garner, L. Boccia, G. Amendola, G. Massa, C. Underwood, M. Brenchley, M. Pointer, M. Sweeting, Antennas for modern small satellites (2009).
[14] J. Ortigosa, N. Padros, M. Iskander, Comparative Study of High Performance GPS Receiving Antenna Designs, IEEE Antennas and Propagation Society, AP-S International Symposium (Digest) 3 (1996) 1958 – 1961.
[15] J. M. Tranquilla, S. R. Best, A study of the quadrifilar helix antenna for global positioning system (gps) applications, IEEE Transactions on Antennas and Propagation 38 (10) (2002) 1545 – 1550.
[16] Saranetel, Sarantel GPS Antenna to Debut in Space on Surrey Satellite Technology's New Miniature Satellite (2010). URL http://www.sarantel.com/press
[17] S. L. M. Markgraf, O. Montenbruck, A Flexible GPS Tracking System for Sub-orbital and Space Vehicles, in: Proceedings of 9th Saint Petersburg International Conference on Integrated Navigation Systems, Saint Petersburg, Russia, 2002.
[18] J. Wertz, W. Larson, Ch. 13, Space Mission Analysis and Design (SMAD), 3rd Edition, Microcosm Press, El Segundo, CA, 1999.
[19] D. Boyd, Calculate the Uncertainty of NF Measurement, Microwaves & RF Magazine. URL http://www.mwrf.com/Globals/PlanetEE/Content/9595.pdf
[20] C. Wang, R. A. Walker, M. P. Moody, A gps signal transmission model for improved single antenna attitude determination, in: Australian International Aerospace Congress, 2005. URL http://eprints.qut.edu.au/2937/
[21] NovAtel, OEMV Family Installation and Operation User Manual OM-20000093, rev. 8 (Aug 2008).
[22] B. Parkinson, J. Silker, Global Positioning System: Theory and Applications, Vol. I, AIAA, 1996.
[23] Antcom, Antcom Passive S-band RHCP and Rx Beidou Antennas: Pictures, Outline Drawings, Specifications (2011). URL http://www.antcom.com/documents/catalogs/PassiveS-BandandBeidouAntennas.pdf
[24] G. B. Carvalho, P. Gustavsson, S. Theil, H. K. Kuga, Standard Ionospheric and Tropospheric Models for GPS on Aerospace Applications: Geometrical Extension, in: Proceedings of AIAA 57th International Astronautical Congress, Vol. 11, Valencia, Spain, 2006, pp. 7262 – 7272.
[25] G. Gerten, Navigation modeling and Operations Space, Control, and User Segments, User Manual (Jan 2007).
[26] J. Springmann, B. Kempke, J. Cutle, H. Bahcivan, Initial Flight Results of the RAX-2 Satellite, in: Proceedings of the 26th Annual Small Satellite Conference, Logan, UT, 2012.